

Integration of ultrasonic tomography with industrial production line for defectoscopy of semi-finished products

Streszczenie. W artykule zaprezentowano zastosowanie ultradźwiękowej tomografii do wykrywania nieciągłości materiałowych w półproduktach przemysłowych. Technika ta, bazująca na sondach piezoelektrycznych, pozwala na bezinwazyjne badanie wnętrza obiektów, takich jak zbiorniki czy rurociągi. Przedstawiono konstrukcję systemu pomiarowego zintegrowanego z linią produkcyjną oraz przedstawiono porównawczą analizę rekonstrukcji obrazów dla komponentów jednorodnych i wadliwych. Przedstawiono porównanie na 3 różnych komponentach.

Abstract. The article presents the application of ultrasonic tomography for detecting material discontinuities in industrial semi-finished products. This technique, based on piezoelectric sensors, allows for non-invasive examination of the interiors of objects such as tanks or pipelines. The design of a measurement system integrated with a production line and a comparative analysis of image reconstruction for homogeneous and defective components are presented. A comparison was made on three different components. (*Integracja tomografii ultradźwiękowej z linią produkcyjną w defektoskopii półproduktów przemysłowych*).

Słowa kluczowe: tomografia ultradźwiękowa, defektoskopia, nieciągłości materiałowe, półprodukty, linia produkcyjna

Keywords: ultrasonic tomography, defectoscopy, material discontinuities, semi-finished products, production line

Introduction

Ultrasonic tomography is one of the non-invasive methods of examining the interior of objects, which is based on the use of sensors placed on the surface of the item under examination. The technique is used both in medicine, where it is used to visualize tissues [1, 2], botany [3, 4], and in industry [5, 6], in particular to examine the interiors of tanks, chemical reactors [7, 8] and pipelines [9]. One of the applications of ultrasonic tomography, using measurements made with piezoelectric sensors, is the ability to detect discontinuities in homogeneous materials [10, 11, 12, 13]. This method, known as defectoscopy, is an important part of the process of quality control of semi-finished and finished products. Defectoscopy most often uses acoustic wave transmitters (piezoelectric probes) operating in the frequency range from 20 kHz to 10 MHz [14].

Three main types of ultrasonic tomography can be distinguished: reflection tomography, which records the reflection of waves and their time of return (TOF) from the internal structures of an object], transmission tomography, which measures the time of fly-through of a wave from the source to the receiver through the examined structure, and hybrid solutions, which combine both techniques. In the case of reflection tomography, if a material defect is detected in the product under study, the reflected waves reach the receiver faster than in the case of homogeneous materials, which makes it possible to precisely determine the distance of the defect from the edge of the object under study [15-17].

It is necessary to solve the inverse problem and develop appropriate image reconstruction algorithms to reconstruct an image of the object's interior from the collected data. One of the most widely used reconstruction methods in ultrasound tomography is the linear back-projection (LBP) method. It involves modeling the transmission of an ultrasound wave through a medium. For each point (x, y) in the image space, the algorithm sums the values of the reflected signals that may have originated from that point, based on the measured time delays of the signal. This process can be reduced to a matrix multiplication operation of the measurement vector and sensitivity matrix [5]. Other approaches include iterative methods that minimize specific objective functions, as well as spline-based back-projection

algorithms, discretization models and artificial intelligence-based algorithms.

This article presents a measurement system installed on an in-line bench and a comparative analysis of image reconstruction for two cases: a homogeneous component and that one containing defects. In addition, the system's ability to detect material discontinuities and the potential for further development to improve the accuracy of identification and localization of defects in test objects are discussed.

Methods

Ultrasound tomography has a high noise level, affecting the quality of measurements, especially with a small number of sensors. Therefore, it is necessary to preprocess the data and properly remove the noise. In defectoscopic measurements, the most common frequency range is from 20 kHz to 10 MHz, although ultrasonic technology allows frequencies as high as 1 GHz. The choice of frequency, and thus wavelength, depends on the physical parameters of the transmission medium, the characteristics of the defect and, in the case of medical applications, the tissues in the area under examination. The developed solution's initial operating frequency was set at 40 kHz. The frequency of the transmitter was crucial in determining the analog path of the signal under investigation. Dedicated timers in a cascaded arrangement were used to control the excitation of the transmitters as high-voltage pulses. Based on measurement practice, the most effective form of excitation turned out to be a five-fold application of a high-voltage pulse in the +72V range.

The measurement system consists of eight ultrasonic transducers arranged in two parallel rows (Fig. 1) along with a PCB tomograph board (Fig. 2).

The measurements were made with a device equipped with two STM32 G4 microcontrollers, which control the operation of 8 UST ultrasonic probes placed parallel to the transport line. The measurement sequence generates an 8x8 array in the form of each-to-any measurements. The analog measurement path begins by sending the signal received from the ultrasonic transducer to a dual low-noise amplifier (LNA) and a variable gain adjustable amplifier (VGA). After amplifying the analog signal, the conditioned

signal passes through a Butterworth low-pass filter. The signal is then passed to a buffer, the function of which is performed by an operational amplifier. In the analog path, the signal is converted to its envelope. The final step in conditioning the analog signal is feeding it into a combiner circuit, which adjusts the signal offset. Once the signal is fully processed and fed in differential form to an analog-to-digital converter (ADC), it is then sent to image reconstruction modules via a Raspberry PI controller and Kafka broker.

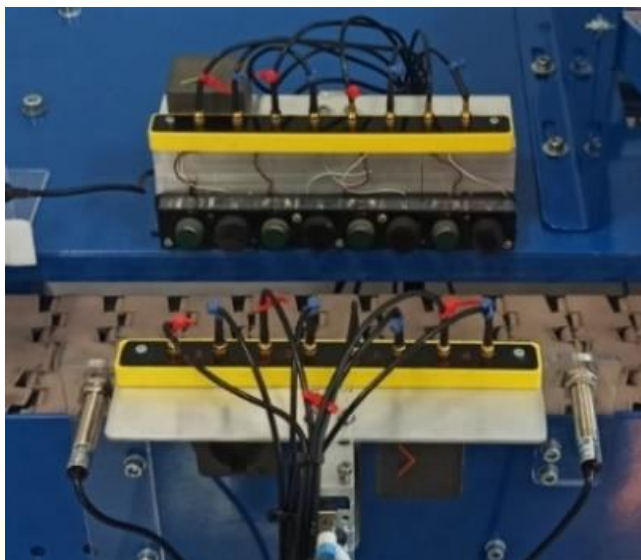


Fig. 1. Semi-industrial ultrasound tomography station - transducer arrangement



Fig. 2. Semi-industrial ultrasonic tomography workstation - tomograph PCB with cover adapted to DIN13 connector.

The model included eight transmitters ($n \in N, |N|=8$) arranged in two parallel lines, four in each, and the measurement taken yielded a vector of 64 values, with those corresponding to the $P(n, n)$ measurement using a mask being zeroed. Reconstruction of the tomographic image can be performed using various algorithms that transform the measurement vector into an image reflecting the spatial distribution of the analyzed parameter by both classical methods and artificial intelligence algorithms. One technique is to solve the inverse problem using the LBP Linear Backprojection algorithm. This algorithm was also chosen in the realization of the described UST platform, and the main criterion for selection was the speed of operation, taking into account the known disadvantages in the form of lower resolution. The method boils down to solving the inverse problem by solving a system of equations, which, by the need for more data than the length of the measurement vector, is an ill-posed problem. It is an underdetermined system of equations. The way to solve it is to use a sensitivity matrix, where a transposed matrix approximates

the inverse matrix, and the reconstruction formula is as follows:

$$\varepsilon = S^T c,$$

where S is the sensitivity matrix and c is the measurement vector. In the system presented here, sound signals in transmission mode are analyzed. The reflected waves used for reflection solutions have been filtered out. In order to develop the sensitivity matrix, an algorithm was prepared to determine the spatial distribution of sound wave propagation. Using a simulation technique, the desired distribution of the parameter was determined for each pair of electrodes, taking into account the geometric characteristics of the measurement space on the production line. Once the reconstructed image was obtained, it was subjected to threshold filtering algorithms to remove irrelevant artifacts and thus sharpen the acquired tomogram. Finally, the data was converted to the range of values displayed in the visualization algorithm using a previously prepared color scale in black and white colors. Due to the undesirable artifacts accompanying a color scale, a monochromatic scale was finally chosen to ensure that the measured value of the tomographic data was maintained.

A comparative study of solid composite blocks and a block with an irregular hole was conducted to assess the ability to detect inhomogeneities in the materials.

Results and discussion

The first experiment aimed at determining the best setting parameters for the measuring device (Table 1). Two parameters of the tomograph settings were configurable: the gain g and the comparator threshold t_c . For the given set of result data, the settings $g=1500$ and $t_c=1925$ were used. These values were determined experimentally as those that allow us to obtain the sharpest result image. Table 1 contains images of the reconstruction variants with the different tomographic set parameters adopted.

Table 1. UST measurement against different settings (vertical view)

g/t_c	Plastic - empty	Epoxide - empty	Epoxide with damage
1500/2000			
1500/1975			
1500/1950			

1500/ 1925			
1500/ 1900			
1500/ 1800			

This was followed by a second experiment comparing the results obtained for two types of measurements: measurement with a reference image and without a reference image. As a result, a set of tomographic images was obtained showing the difference in the distribution of the analyzed parameter for the different phantoms used: empty epoxy phantom, plastic empty phantom, and complete epoxy phantom with defect (Table 2).

Table 2. UST measurement for three phantoms including: epoxy phantom empty, plastic phantom empty, full epoxy phantom with defect (top tomograms - with reference measurement, bottom measurements without reference measurement)

Measurement without references		
Measurement with reference		

The results, despite the fact that they do not give precise information on the observable spatial changes of the reconstructed parameter on the basis of TOF vectors, allow for obtaining necessary information from the point of view of the production process. There are noticeable differences in the identifiable patterns of enhancement of the analyzed spatial variable. The spatial distribution of the TOF disturbance factor, and thus the determination of the precise state of the studied object is difficult to estimate. It was possible to obtain observations: there is a difference between the distribution of the parameter for two types of phantoms (empty phantom - epoxy, empty phantom - plastic), the amplifications between the selected transmitters are different for the empty phantom, as well as slight differences were noted for the full damaged phantom.

The third experiment estimated the repeatability of the results by performing numerous measurement sequences. The results were positive. A tomographic image averaging algorithm was also applied for the indicated phantoms. The results confirm the existence of reproducible patterns of the obtained images with respect to the type of object located in the sensor measurement space, as confirmed by the graphics in Table 3.

Table 3. Averaging of tomographic images for successive phantoms used.

Phantom empty - resin	Phantom empty-plastic	Phantom full epoxy with defect

In addition, a study of changes in the analyzed spatial parameter as a function of the phantom's position in the UST sensor's measurement space was carried out. The device's ability to detect the correctness of the object's location in the measurement area was confirmed, as shown in Table 4.

Table 4. Analysis of reconstructed UST images as a function of phantom position on the production line.

Partial phantom placement position	The half-phantom placement position	Full phantom placement position

The experiments performed indicate the possibility of detecting material discontinuities in the longitudinal section of the phantom, although the results have low detail. They depend significantly on the number of transmitters, the reconstruction algorithm, and reconstruction parameters such as the sensitivity matrix. The ongoing work requires continuation and further, deeper research. There is a need to develop the developed tomographic tool.

Conclusion

The research demonstrates the potential of ultrasonic tomography in detecting material discontinuities, particularly in industrial applications. The study successfully highlighted differences in material homogeneity and defects by utilizing an array of eight ultrasonic transducers and implementing the Linear Back Projection (LBP) algorithm for image reconstruction. The experiments conducted on various types of phantom blocks (solid, plastic, and defective) showed that ultrasonic tomography can provide valuable spatial insights into material integrity. Although the results indicated certain limitations in spatial resolution and the ability to precisely identify the location of defects, the system's repeatability and ability to detect changes in the tested materials were confirmed.

However, the study also identified several challenges, such as the influence of noise, the need for optimization of measurement parameters (like gain and comparator threshold), and the impact of the number of transducers on image quality. The selected frequency of 40 kHz and the experimental setup provided useful results, but there is a significant room for improvement in terms of accuracy and defect localization. Further development of the ultrasonic tomography system, including refining algorithms and increasing the number of sensors, could significantly enhance its capabilities. The results suggest a promising future for this technology in industrial and medical applications, provided that the continued research and optimization efforts are pursued.

Autorzy: Krzysztof Król M.Sc., Faculty of Transport and Computer Science, WSEI University, Projektowa 4, 20-209 Lublin, Poland, Research&Development Centre Netrix S.A. Związkowa 26, 20-148 Lublin, Email: krzysztof.krol@netrix.com.pl; Grzegorz Rybak, Ph.D. Research&Development Centre Netrix S.A. Związkowa 26, 20-148 Lublin, Email: grzegorz.rybak@netrix.com.pl; Dariusz Majerek, Ph.D. Lublin University of Technology, Nadbystrzycka 38, Lublin, Poland Email: d.majerek@pollub.pl, Poland, Bartosz Przysucha Ph.D. Lublin University of Technology, Nadbystrzycka 38, Lublin, Poland E-mail: b.przysucha@pollub.pl; Konrad Niderla M.Sc. Faculty of Transport and Computer Science, WSEI University, Projektowa 4, 20-209 Lublin, Poland, Research&Development Centre Netrix S.A. Związkowa 26, 20-148 Lublin, Email: konrad.niderla@netrix.com.pl;

LITERATURA

- [1] Huang, J., Lin, Y., Zhang, Z., Labyed, Y., Tan, S. Breast ultrasound waveform tomography: using both transmission and reflection data, and numerical virtual point sources. *SPIE Medical Imaging: Ultrasonic Imaging and Tomography*, 2014.
- [2] Ruitter, N. V., Zapf, M., Hopp, T., Gemmeke, H. Quantitative Ultrasound in Soft Tissues. In *Ultrasound Tomography* (pp. 171–200). *Advances in Experimental Medicine and Biology*, volume 1403. Springer, 2023.
- [3] Espinosa, L., Brancheriau, L., Cortes, Y., et al. Ultrasound computed tomography on standing trees: accounting for wood anisotropy permits more accurate detection of defects. *Annals of Forest Science*, 77 (2020), No.68
- [4] Korzeniewska, E., Sekulska-Nalewajko, J., Gocawski, J., Drożdż, T., Kiebasa, P. Analysis of changes in fruit tissue after the pulsed electric field treatment using optical coherence tomography. *EPJ Applied Physics*, 91 (2020), No. 3, 30902
- [5] Baran B, Kozłowski E, Majerek D, Rymarczyk T, Soleimani M, Wójcik D. Application of Machine Learning Algorithms to the Discretization Problem in Wearable Electrical Tomography Imaging for Bladder Tracking, *Sensors*, 23 (2023); No. 3,1553
- [6] Przysucha B, Wójcik D, Rymarczyk T, Król K, Kozłowski E, Gąsior M. Analysis of Reconstruction Energy Efficiency in EIT and ECT 3D Tomography Based on Elastic Net. *Energies*, 16 (2023); No. 3, 1490
- [2] Król, K., Rymarczyk, T., Niderla, K., & Kozłowski, E., Sensor platform of industrial tomography for diagnostics and control of technological processes. *Informatyka, Automatyka, Pomiary W Gospodarce I Ochronie Środowiska*, 13 (2023), No.1, 33–37
- [8] Cailly, W., Walaszek, H., Brzuchacz, S., Zhang, F., Lasaygues, P. Pipe two-phase flow non-invasive imaging using Ultrasound Computed Tomography: A two-dimensional numerical and experimental performance assessment. *Flow Measurement and Instrumentation*, 74, August 2020, 101784
- [9] Chen, J., Fei, C., Lin, D., Gao, P., Zhang, J., Quan, Y., Chen, D., Li, D., Yang, Y. A Review of Ultra-High Frequency Ultrasonic Transducers. *Frontiers in Materials*, 2020
- [10] Kulisz M, Kłosowski G, Rymarczyk T, Stoniec J, Gauda K, Cwynar W. Optimizing the Neural Network Loss Function in Electrical Tomography to Increase Energy Efficiency in Industrial Reactors. *Energies*, 17 (2024); No. 3, 681
- [11] Xu, X., Ran, B., Jiang, N., Xu, L., Huan, P., Zhang, X., Li, Z. A systematic review of ultrasonic techniques for defects detection in construction and building materials. *Measurement*, 226 (2024), 114181
- [12] Zhang, Q., Peng, J., Tian, K., Wang, A., Li, J., Gao, X. Advancing Ultrasonic Defect Detection in High-Speed Wheels via UT-YOLO. *Sensors*, 24 (2024),1555
- [13] Kłosowski G, Rymarczyk T, Niderla K, Kulisz M, Skowron Ł, Soleimani M. Using an LSTM network to monitor industrial reactors using electrical capacitance and impedance tomography – a hybrid approach, *Eksploatacja i Niezawodność – Maintenance and Reliability*, 25 (2023). No.1
- [14] Wiskin, J., Malik, B., Klock, J. Low-frequency 3D transmission ultrasound tomography: technical details and clinical implications. *Zeitschrift für Medizinische Physik*, 33 (2023), No.3, 427-443
- [15] Szabo, T. L., Kaczkowski, P. *Essentials of Ultrasound Imaging*. Elsevier Science, 2023.
- [16] Soleimani M., Rymarczyk T., Kłosowski G., Ultrasound Brain Tomography: Comparison of Deep Learning and Deterministic Methods, *IEEE Transactions on Instrumentation and Measurement*, 73 (2024), 4500812
- [17] Maciura, Łukasz, Wójcik, D., Rymarczyk, T., Król, K., Novel hybrid algorithm using convolutional autoencoder with SVM for electrical impedance tomography and ultrasound computed tomography. *Informatyka, Automatyka, Pomiary W Gospodarce I Ochronie Środowiska*, 13 (2023), No. 2, 4–9